



Published in final edited form as:

*Nat Commun.* ; 6: 7087. doi:10.1038/ncomms8087.

## Muscle stem cells contribute to myofibers in sedentary adult mice

Alexandra C. Keefe<sup>1,4</sup>, Jennifer A. Lawson<sup>1,4</sup>, Steven D. Flygare<sup>1</sup>, Zachary D. Fox<sup>1</sup>, Mary P. Colasanto<sup>1</sup>, Sam J. Mathew<sup>1,2</sup>, Mark Yandell<sup>1,3</sup>, and Gabrielle Kardon<sup>1,\*</sup>

<sup>1</sup>Department of Human Genetics, University of Utah, Salt Lake City, UT 84112 USA

<sup>3</sup>USTAR Center for Genetic Discovery, University of Utah, Salt Lake City, UT 84112

### Abstract

Skeletal muscle is essential for mobility, stability, and whole body metabolism, and muscle loss, for instance during sarcopenia, has profound consequences. Satellite cells (muscle stem cells) have been hypothesized, but not yet demonstrated, to contribute to muscle homeostasis and a decline in their contribution to myofiber homeostasis to play a part in sarcopenia. To test their role in muscle maintenance, we genetically labeled and ablated satellite cells in adult sedentary mice. We demonstrate via genetic lineage experiments that even in the absence of injury, satellite cells contribute to myofibers in all adult muscles, although the extent and timing differs. However, genetic ablation experiments showed that satellite cells are not globally required to maintain myofiber cross-sectional area of uninjured adult muscle.

### INTRODUCTION

Skeletal muscle is critical for locomotion, structural support, and regulation of whole body metabolism. Consequently, homeostatic maintenance of muscle mass is essential for muscle function, and pathological loss of muscle has profound negative consequences<sup>1</sup>. During aging, even in otherwise healthy individuals, muscle mass and function are progressively lost, in a process termed sarcopenia<sup>1,2</sup>. Sarcopenia strongly affects quality of life by impairing locomotion, increasing the likelihood for injury, and increasing the risk of insulin resistance and type 2 diabetes<sup>1</sup>. Thus, an understanding of the requirements for maintaining muscle homeostasis is a critical human health need.

Users may view, print, copy, and download text and data-mine the content in such documents, for the purposes of academic research, subject always to the full Conditions of use:[http://www.nature.com/authors/editorial\\_policies/license.html#terms](http://www.nature.com/authors/editorial_policies/license.html#terms)

Author for correspondence. [gkardon@genetics.utah.edu](mailto:gkardon@genetics.utah.edu), 801 585-6184 phone, 801 581-7996 fax.

<sup>2</sup>Current address: Regional Centre for Biotechnology, Gurgaon, India 122016

<sup>4</sup>These authors contributed equally to this study

#### AUTHOR CONTRIBUTIONS

A.C.K., J.A.L., and G.K. designed the study. A.C.K., J.A.L., Z.D.F., M.P.C., S.J.M. performed experiments and collected the data. S.D.F. and M.Y. developed MuscleQNT. A.C.K., J.A.L., S.D.F., M.Y., and G.K. analyzed the data. A.C.K. and G.K. wrote the manuscript. All authors approved the final version of the manuscript.

#### COMPETING FINANCIAL INTERESTS

The authors declare no competing financial interests.

Muscle is composed of multinucleate myofibers, and all myonuclei are terminally post-mitotic. Maintenance of muscle mass requires conservation of both the number and size of myofibers, and the number of myonuclei in a myofiber is an important regulator of myofiber size<sup>3</sup>. During sarcopenia, loss of muscle mass is due to both a loss of myofibers and a decrease in myofibers' cross-sectional area (CSA), with fast contracting myofibers and hind limb muscles (in humans, mice, and rats) being particularly vulnerable<sup>1,4</sup>. The mechanisms regulating muscle homeostasis and sarcopenia are complex and involve regulation of protein turnover by motor neurons, hormones, immune signals, nutrition, and physical activity<sup>1</sup>.

Adult muscle contains a population of resident stem cells, called satellite cells, and an important unresolved question is whether satellite cells play a role in muscle homeostasis and sarcopenia<sup>4-7</sup>. Genetic labeling and ablation studies have definitively established that satellite cells are the endogenous stem cells necessary and sufficient for muscle regeneration<sup>8-10</sup> and that they contribute to muscle hypertrophy as well<sup>11</sup>. In the absence of injury, satellite cells are thought to be quiescent and both myonuclear and myofiber number invariant<sup>4</sup>, but a limited number of studies indicate that new myonuclei are added to uninjured myofibers<sup>12-14</sup>. Because myonuclei are post-mitotic, this suggests that satellite cells contribute myonuclei during homeostasis. During aging, multiple studies show that myonuclei are lost<sup>3,15-17</sup>, leading to myofiber atrophy<sup>3</sup>, and suggest that in sarcopenia satellite cell replenishment of myonuclei may be inadequate. However, neither the hypothesis that satellite cells contribute to muscle homeostasis nor the hypothesis that a decline in satellite cell-mediated replenishment of myonuclei contributes to sarcopenia has been explicitly tested.

In this study, we use mouse genetics to specifically label or ablate satellite cells to test their role in muscle homeostasis. We demonstrate via genetic lineage experiments that during adulthood satellite cells contribute to uninjured myofibers in all muscles, including hind limb, diaphragm, and extraocular (EOM) muscles. However, genetic ablation experiments showed that satellite cells are not globally required to maintain myofiber cross-sectional area of uninjured adult muscle.

## RESULTS

### Satellite cell number differs between muscles and with age

The number of satellite cells resident in a particular muscle is potentially an important determinant of a muscle's ability to maintain homeostasis. Multiple studies report that satellite cells differ between anatomical muscles<sup>18-22</sup>, are enriched in muscles with slow MyHCI myofibers<sup>17,19,20,22</sup>, and vary with age<sup>23</sup>. Cross-comparison of these studies has been hampered by the use of different species at diverse ages, and the use of different satellite cell markers and methodologies for quantification. To date, no single study has compared the number of satellite cells in multiple muscles concurrently and over time.

To explicitly compare satellite cell numbers in different muscles, we examined five hind limb muscles, the diaphragm, and EOMs of adult male mice. We focused on hind limb muscles because these are highly susceptible to sarcopenia in humans and mice<sup>1,3,15,24-26</sup>. We examined the extensor digitorum longus (EDL), which is highly enriched in fast

(myosin heavy chain MyHCIIb+) myofibers; the soleus, which has > 50% slow (MyHCI+) myofibers<sup>27,28</sup>; and the tibialis anterior (TA), gastrocnemius, plantaris, which are composed of a range of myofiber types<sup>27,28</sup>. Additionally, the diaphragm and EOMs were included because their molecular characteristics, morphology, function, innervation, and aging are distinct from limb muscles<sup>21,29,30</sup>. We first analyzed satellite cell content in sedentary 12 month male mice (this represents 46% of mean lifespan, based on average lifespan of 26 months for C57/B16J mice) an age when muscle growth is complete<sup>31</sup> and myofiber number and CSA have not been reported to decline. Sedentary mice were chosen to represent a “ground”, unexercised state (without acute or intentional injuries), and only males were analyzed to minimize sex-specific differences. Satellite cells were identified and quantified on sections by Pax7, a transcription factor that specifically and robustly marks satellite cells in adult and aged mice<sup>22,32</sup>. We found that most limb muscles (EDL, TA, gastrocnemius, plantaris) had similar numbers of satellite cells, approximately 2000 cells/mm<sup>3</sup> (Fig. 1a–d). The soleus and diaphragm muscles, which are enriched in slow myofibers, had 5000 and 5700 cells/mm<sup>3</sup>, respectively (Fig. 1e–f). EOMs had the greatest number of satellite cells, 9800 satellite cells/mm<sup>3</sup>, potentially correlating with the higher density of myofibers in this muscle (Fig. 1g). Thus, satellite cell density varies nearly 5-fold between muscles in the adult mouse.

To test whether satellite cell number changes over time, we quantified Pax7+ satellite cells at 20 months (77% of mean lifespan), a time at which sarcopenia of limb muscles has not been reported in mice<sup>3,25</sup>. Most limb muscles (EDL, TA, plantaris, soleus) had no change in satellite cell number at 20 months (Fig. 1a, b, d, e). However, in the gastrocnemius, diaphragm, and EOMs, satellite cell numbers significantly declined 16–22% (Fig. 1c, f, g).

### Satellite cells contribute to myofibers in all adult muscles

To test whether satellite cells contribute to myofibers during muscle homeostasis, we genetically labeled and followed the long-term fate of satellite cells in uninjured adult muscle (Fig. 2a). Satellite cells were labeled using *Pax7<sup>CreERT2</sup>*, an allele that we previously demonstrated specifically and efficiently induces recombination in > 95% of Pax7+ satellite cells after delivery of tamoxifen (TAM)<sup>9</sup>. We crossed these mice to the *Rosa<sup>mTmG</sup>* reporter, which ubiquitously expresses membrane-bound Tomato, until Cre-mediated recombination excises *Tomato* and results in membrane-bound GFP expression<sup>33</sup>. We generated male *Pax7<sup>CreERT2/+</sup>;Rosa<sup>mTmG/+</sup>* mice, labeled satellite cells at 6 months, via TAM, and harvested muscles at 12 or 20 months. In these mice, the presence of GFP+ myofibers indicates at least one satellite cell contributed to those myofibers between 6–12 or 6–20 months. In the absence of TAM, *Rosa<sup>mTmG/+</sup>* mice had no GFP+ myofibers (Supplementary Fig. 1d) and *Pax7<sup>CreERT2/+</sup>;Rosa<sup>mTmG/+</sup>* mice had few GFP+ myofibers at 12 or 20 months (0–5.3% GFP/total myofibers; Supplementary Fig. 1), confirming that the *Pax7<sup>CreERT2</sup>* allele is tightly TAM-regulated.

In all muscles examined at 12 or 20 months, GFP+ myofibers were present, which indicates that at least one satellite cell contributed to these myofibers (Fig. 2). In longitudinal sections, GFP was often expressed along regions of the myofiber greater than 950 μm in length (Fig. 2b). Given that gene products from a single myonucleus have been measured to spread 200

$\mu\text{m}^{34}$  and up to  $1000 \mu\text{m}^{35}$  along the length of a myofiber, this suggests that potentially more than 1 satellite cell contributed to some GFP+ myofibers. Interestingly, while centralized myonuclei are a hallmark of satellite-cell mediated regenerated myofibers<sup>18</sup>, less than 1% of the GFP+ myofibers had centrally localized myonuclei (Fig. 2c).

The degree of satellite cell contribution to myofibers between 6 and 12 months differed between muscles (Fig. 2). In limb muscles, 8–36% of the myofibers were GFP+ (Fig. 2d–i), and in the diaphragm and EOM 31% and 18% of myofibers were GFP+, respectively (Fig. 2k, m). Within individual muscles, the anatomical location of GFP+ myofibers varied: GFP+ myofibers were more prevalent in regions closer to the bone for the TA and gastrocnemius and in the global region of EOMs, but showed no positional bias in other muscles (Supplementary Fig. 1). The diaphragm and soleus muscles contained 10% and 55% slow MyHCI+ myofibers (Fig. 2h). Satellite cells contributed equally to slow and fast myofibers in the diaphragm, but contributed preferentially to fast myofibers in the soleus (Fig. 2j, l). Thus, while satellite cells contributed to all muscles between 6 and 12 months, the degree of contribution differed between muscles, within muscles, and by fiber type.

Examination of muscles at 20 months revealed that between 12 and 20 months satellite cells only continued to contribute to myofibers in a subset of muscles. In the EDL, TA, plantaris, and soleus, the percentage of GFP+ myofibers did not significantly change from 12 to 20 months (Fig. 2d, e, g, i), indicating that satellite cells did not measurably contribute to additional myofibers after 12 months. In the gastrocnemius and EOM, the percentage of GFP+ myofibers increased (Fig. 2f, m), demonstrating that satellite cells contributed to an average of 1–2% of myofibers per month between 12 and 20 months (assuming continuous contribution). The diaphragm had the largest increase in GFP+ myofibers, indicating continued satellite cell contribution at a rate of 5% of myofibers per month (assuming continuous contribution; Fig. 2k). As in the 12-month cohort, satellite cells continued to contribute equally to diaphragm slow and fast myofibers. An examination of satellite cell contribution across muscles in individual mice in the 20 month cohort revealed variability between animals: one mouse had consistently high and another mouse had consistently low levels of satellite cell contribution in multiple muscles ( $p < 0.003$ , Supplementary Fig. 2), despite the mice being littermates, housed together, and receiving saturating levels of TAM. Together these results demonstrate that satellite cells contribute to the myofibers of all adult muscles in the absence of injury, although the extent, distribution, rate, and timing of contribution vary between muscles and animals.

### **By 20 months myofibers decline in size in most limb muscles**

Myofiber CSA has been shown to decline in humans<sup>17,36,37</sup> and mice<sup>3,15,25,38</sup> with advanced age. Our evidence of satellite cell contribution to adult uninjured myofibers suggests that satellite cells may be important for replenishment of aging myonuclei and ultimately maintenance of myofiber CSA. We therefore quantified the CSA of individual myofibers in control muscles at 12 and 20 months.

To quantify CSA of myofibers throughout an entire muscle, we used our newly developed analytical tool, MuscleQNT<sup>39</sup>. Muscles were harvested at 12 and 20 months from control male mice, sectioned, and myofibers labeled with antibodies to laminin and slow MyHCI

and analyzed with MuscleQNT. MuscleQNT applies an adaptive thresholding method to locate myofiber boundaries and then erosion and dilation steps to isolate and quantify CSA of individual myofibers. Thus MuscleQNT enables the unbiased, automated quantification of all myofibers in a muscle cross-section. It is best used for explicit comparison of two data sets analyzed using identical input parameters, as CSA values are highly dependent on these parameters. Therefore, we analyzed sections of 12 and 20 month control muscles using identical input parameters (parameters for each muscle are listed in Supplementary Table 2). For each muscle we generated histograms of 12 and 20 month myofiber CSA and determined whether the frequency of the myofibers in each bin was significantly different between 12 and 20 months via permutation tests (see **Methods**). We also tested for each muscle whether the overall size of myofibers was significantly different between the different aged cohorts using a hierarchical linear model with a random effect to control for intra-class correlation among measured myofibers within individual animals.

Analysis at 12 months showed that myofiber size differed considerably between the muscles (Fig. 3, Supplementary Fig. 3). The mean myofiber size in limb muscles ranged from 750 to 1090  $\mu\text{m}^2$  (Fig. 3a–e, Supplementary Fig. 3a). The mean diaphragm myofiber size was smaller (420  $\mu\text{m}^2$ , Fig. 3f, Supplementary Fig. 3a), and EOM myofibers were the smallest and most tightly constrained in size (120  $\mu\text{m}^2$ , Fig. 3g, Supplementary Fig. 3a).

Surprisingly, comparison of 12 and 20 month muscles revealed that in most limb muscles of older animals myofibers were already smaller (Fig. 3, Supplementary Fig. 3), although in mice sarcopenia has been described as beginning at 24–26 months<sup>3,15,24,26</sup>. In the diaphragm the distribution of myofiber sizes and average myofiber size were unaffected with age (Fig. 3a, f, Supplementary Fig. 3a). In contrast, in the TA, gastrocnemius, plantaris, and soleus myofibers had shifted towards significantly smaller sizes (Fig. 3b–e, Supplementary Fig. 3a). In the plantaris, this shift resulted in a significantly smaller total muscle cross-sectional area (Supplementary Fig. 3b). In the soleus, the shift to smaller myofibers occurred in both fast and slow myofibers. Finally, in the 20 month EOMs the majority of myofibers shifted to smaller sizes, while a minority of myofibers hypertrophied (possibly in compensation, Fig. 3g, Supplementary Fig. 3a).

### Satellite cells are not required globally for maintenance of adult myofiber area

Our analysis unexpectedly shows that by 20 months myofibers in most limb muscles are undergoing an age-related decline in myofiber CSA. We also find that satellite cells contribute significantly to all muscles during this time. Therefore we hypothesized that satellite cells may be critical for maintenance of myofiber size. If this hypothesis is correct, ablation of satellite cells should lead to smaller myofibers and potentially exacerbate the decline in CSA seen in most muscles at 20 months.

To test the role of satellite cells in maintenance of myofiber size, we genetically ablated satellite cells using *Pax7<sup>CreERT2/+</sup>;Rosa<sup>DTA/+</sup>* mice (Fig. 4a). In these mice, Cre activates expression of diphtheria toxin A (DTA) and specifically kills Pax7<sup>+</sup> satellite cells in response to TAM<sup>40,41</sup>. Satellite cells were ablated in male *Pax7<sup>CreERT2/+</sup>;Rosa<sup>DTA/+</sup>* mice via TAM at 6 months and harvested at either 12 or 20 months. Male *Pax7<sup>+/+</sup>;Rosa<sup>DTA/+</sup>* littermates given TAM were used as controls. In *Pax7<sup>CreERT2/+</sup>;Rosa<sup>DTA/+</sup>* mice given

TAM, satellite cells were ablated with > 97% efficiency in all muscles (Supplementary Fig. 4). Again, we used Muscle QNT to analyze myofiber CSA using input parameters empirically determined for each cohort of 12 month or 20 month control and satellite cell ablated muscles (see parameters in Supplementary Table 2).

Ablation of satellite cells variably affected different muscles. In most limb muscles (TA, gastrocnemius, plantaris, soleus) at 12 or 20 months there was no difference in average myofiber sizes or their distribution with satellite cell ablation (Fig. 4c–g, Supplementary Fig. 5). In the diaphragm, satellite cell ablation had no effect on the majority of myofibers (which are fast) at 12 or 20 months, but slow myofibers shifted to smaller sizes at 12 months (Fig. 5a–b, Supplementary Fig. 5). Interestingly, in the EOMs satellite cell ablation had no effect at 20 months, but at 12 months resulted in smaller myofibers (seen in shift in distribution of myofibers, but not in overall average size; Fig. 5c, Supplementary Fig. 5). In addition, while satellite cell ablation had no effect on the size of myofibers in the EDL at 12 months, at 20 months ablation resulted in a shift towards smaller myofibers and a significant 15% decline ( $p = 0.049$ ) in average myofiber size (Fig. 4b, Supplementary Fig. 5).

The observation that satellite cell ablation had an effect on the EDL, but a relatively minor effect on the diaphragm was unexpected. In the EDL, satellite cells only appreciably contributed to 30% of myofibers prior to 12 months. In contrast, in the diaphragm satellite cells continuously contributed to myofibers, with 75% of myofibers having received satellite cell-derived myonuclei by 20 months. If satellite cell contribution is important for myonuclear replenishment, we reasoned that the difference in the effect of satellite cell ablation on EDL versus the diaphragm might be explained by a difference in myonuclear dynamics; satellite cell-mediated replenishment of myonuclei may only be functionally important in muscles where the number of myonuclei are declining.

To test for changes in myonuclear number, we quantified the number of myonuclei in control and satellite cell ablated diaphragms, EDL, and also the plantaris (which was unaffected by satellite cell ablation, but suffered satellite cell-independent decline in myofiber CSA) at 12 and 20 months. To control for age-related changes in myonuclear size<sup>3</sup>, we quantified the myonuclear length from longitudinal sections of these muscles and applied a correction factor to our myonuclear counts<sup>42</sup>. We found that between 12 and 20 months in the diaphragm and plantaris the number of myonuclei did not decline, even in the absence of satellite cell contribution (Fig. 4h, 5d). In contrast, in the EDL there was a significant 25% loss of myonuclei between 12 and 20 months in control mice ( $p < 0.05$ ; Fig. 4h). The decline in myonuclei between 12 and 20 months in ablated mice demonstrates that EDL myofibers suffer myonuclear decline independent of satellite cells. However, comparison of control and satellite cell ablated mice at either 12 or 20 months shows that the presence of satellite cells did not detectably affect myonuclear numbers in EDL myofibers.

## DISCUSSION

Satellite cells are the endogenous resident stem cells uniquely capable of replacing post-mitotic myonuclei and myofibers in the adult. It is well established that these stem cells are necessary and sufficient for regeneration of damaged myofibers<sup>8,10,41</sup>. However, satellite

cells also have been hypothesized to contribute to muscle homeostasis and a decline in satellite-cell mediated replenishment of myonuclei may contribute to sarcopenia<sup>5,7</sup>.

By genetically labeling and following the long-term fate of satellite cells, we demonstrate for the first time that satellite cells contribute to myofibers in all adult muscles in the absence of injury (Fig. 6). The extent of this satellite cell addition varies widely between and within muscles and with age. After 12 months, satellite cells ceased to contribute to myofibers of most hind limb muscles, but not in the gastrocnemius, diaphragm, and EOMs. Strikingly, only in these three muscles did the number of satellite cells decline with age. Thus, continued satellite cell contribution during homeostasis appears to deplete the pool of resident, quiescent satellite cells.

The substantial contribution of satellite cells to myofibers to adult uninjured myofibers raises the question: What signals recruit satellite cells? The signal is unlikely to be myonuclear loss. Our findings that satellite cells do not contribute to EDL myofibers after 12 months despite a clear loss of myonuclei and that, conversely, satellite cells continuously contribute to diaphragm myofibers that maintain a stable number of myonuclei contradict such a hypothesis. Our data do indicate that the signals are likely to be dynamic and both local and systemic. Satellite cell contribution varies over time and between muscles, within muscles, and between fiber types, and this suggests that local signals within the muscles dynamically regulate recruitment of satellite cells. Furthermore, our observation that a few mice had higher or lower levels of satellite cell contribution across most muscles implicates the presence of systemic signals, perhaps related to the recently described  $G_{Alert}$  signals<sup>43</sup> that globally modulate satellite cell recruitment to uninjured myofibers. Alternatively, this inter-animal variation may reflect differences in activity levels or other behavioral parameters. Determining the biomechanical, cellular, and molecular signals regulating satellite cell recruitment will be an important area of future research.

Our experiments genetically ablating satellite cells in uninjured mice explicitly test whether satellite cell contribution is critical for maintenance of adult myofiber size (Fig. 6). In most limb muscles (TA, gastrocnemius, plantaris, and soleus) satellite cells were not required for maintenance of myofiber cross-sectional area, although by 20 months these muscles suffered a satellite cell-independent decline of myofiber size. Surprisingly, despite high and continuous contribution of satellite cells to myofibers, diaphragm myofibers also did not require satellite cells for maintenance of myofiber size (with the exception of slow myofibers, which constitute only 10% of myofibers, at 12 months). However, the stability of myonuclear numbers in the diaphragm between 12 and 20 months suggests that myonuclear replenishment may not be required during this time. A requirement for satellite cell contribution in diaphragm and the 4 limb muscles may only become manifest in older (e.g. 24 month) mice.

EOMs are unique amongst skeletal muscles in having continuous myonuclear addition throughout life<sup>12,44</sup>. Consistent with these previous reports, we found that satellite cells continuously contributed to EOM myofibers. In addition, ablation of satellite cells shifted the distribution of EOM myofiber cross-sectional area to smaller sizes at 12 months, suggesting that satellite cell contribution may be important. By 20 months, satellite cells

appeared not to be required for myofiber maintenance. However, unlike other skeletal muscles, there is evidence that EOMs contain another population of satellite cells that are Pax7-Pitx2<sup>+</sup><sup>45</sup>, and Pitx2 is required for development and maintenance of EOMs<sup>46–49</sup>. Thus, this alternative Pax7-satellite cell population may compensate in the older mice lacking Pax7<sup>+</sup> satellite cells, a hypothesis to be tested in future experiments.

In mouse, the EDL is largely composed of fast MyHCIIb myofibers, and this muscle is particularly susceptible to myonuclear apoptosis, atrophy, and neuromuscular dysfunction with age<sup>15,50–52</sup>. Consistent with these reports, we found that the EDL suffered a decline in myonuclear number between 12 and 20 months. Our lineage studies showed that satellite cells contributed to 30% of EDL myofibers prior to 12 months. Despite this modest contribution, ablation of satellite cells lead to a decline in myofiber cross-sectional area at 20 months. How satellite cells may play a role in maintaining EDL myofiber size is currently unclear. The most obvious hypothesis is that satellite cells replenish declining numbers of myonuclei. However, comparison of satellite cell-ablated versus control 20 month EDL muscles did not reveal a significant rescue of myonuclei when satellite cells were present.

Satellite cells are required for regeneration and we now also show they contribute to uninjured adult myofibers. Intriguingly, our work suggests that the mechanisms regulating satellite cells' contribution to regenerating and uninjured myofibers may differ significantly. First, self-renewal of satellite cells is an important property of regeneration, but in muscles with continuous satellite cell contribution to uninjured myofibers the satellite cell pool is not maintained. Second, a hallmark of regenerated myofibers is the presence of centralized myonuclei. However, despite the presence of many uninjured myofibers to which satellite cells had contributed, we found few centralized myonuclei (see also<sup>22</sup>). Dysregulation of satellite cells may also play a role in sarcopenia. A decline in satellite cell-mediated regeneration with age has been widely recognized<sup>23</sup>. Additionally, a decline in satellite cell contribution to uninjured myofibers may contribute to sarcopenia. Recent satellite cell ablation studies<sup>53</sup> found that depletion of satellite cells did not accelerate or exacerbate sarcopenia in aged mice. However, in this study satellite cell ablation was incomplete (ranged from 64–87%) and in our study we have not explicitly tested the role of satellite cells in uninjured muscle of aged (e.g. 24 month) mice. Future satellite cell lineage and ablation studies of uninjured and exercised aged mice will be essential to establish whether a decline in satellite cell contribution to myofibers plays a role in sarcopenia.

## METHODS

### Mice and Tamoxifen delivery

All mouse lines were previously reported: *Pax7<sup>CreERT241</sup>*; *Rosa<sup>mTmG33</sup>*, and *Rosa<sup>DTA/+40</sup>*. *Pax7<sup>CreERT2</sup>* mice were backcrossed > 8 generations onto C57BL/6J background. Only male mice were used, and at least 5 mice were used for each cohort in control and ablation studies. At 6 months of age, satellite cell-labeled (*Pax7<sup>CreERT2/+</sup>*; *Rosa<sup>mTmG/+</sup>*, n = 4 at 12 months, n = 6 at 20 months), satellite cell-ablation (*Pax7<sup>CreERT2/+</sup>*; *Rosa<sup>DTA/+</sup>*, n = 8 at 12 months, n = 6 at 20 months), and littermate control (*Pax7<sup>+/+</sup>*; *Rosa<sup>DTA/+</sup>*, n = 7 at 12 months, n = 5 at 20 months) mice were given five, 10 mg doses (50 mg total) of Tamoxifen (TAM) by gavage. To ensure continuous ablation/labeling, additional 10 mg doses were given once



per month until 12 months, and mice were subsequently harvested at 12 or 20 months. Additionally, a small cohort of *Pax7<sup>CreERT2/+</sup>;Rosa<sup>mTmG/+</sup>* mice was housed separately, not given TAM, and harvested at 12 or 20 months. It was noted that long-term TAM treatment led to inguinal hernias in some mice as has been reported previously<sup>54</sup>, though this phenotype was observed in equal ratios in control and mutant cohorts. All mice were otherwise healthy at harvest. Mice were housed in the University of Utah animal facility located at 5000 ft elevation, and this relatively high elevation may contribute to the early onset of satellite-cell independent sarcopenia in the mice. No statistical method was used to predetermine sample size; all animals were included; and the experiments were not randomized. Animal experiments were performed in accordance with protocols approved by the Institutional Animal Care and Use Committee at the University of Utah.

### Immunofluorescence and microscopy

Extensor digitorum longus (EDL), tibialis anterior (TA), gastrocnemius, plantaris, soleus, diaphragm and extraocular (EOM) muscles from each animal were harvested, flash-frozen, and sectioned at 8 or 12  $\mu\text{m}$  (cross-sections) or 20  $\mu\text{m}$  (longitudinal sections). For section immunofluorescence, slides were fixed in 4% PFA for 5 minutes, washed in 1 $\times$  PBS, and then if needed (see Supplementary Table 1), subjected to antigen retrieval (heated in 1.8mM citric acid, 8.2 mM sodium citrate in H<sub>2</sub>O in a 2100 PickCell Retriever). Sections that required tyramide signal amplification (TSA) were quenched in 3% H<sub>2</sub>O<sub>2</sub> for 5 minutes. All slides were blocked in 5% serum or 0.5% TNB blocking reagent (PerkinElmer) in 1 $\times$  PBS for 60 min, and incubated in 1 $^{\circ}$  antibody (Supplementary Table 1) overnight at 4 $^{\circ}\text{C}$ . Slides were washed in 1 $\times$  PBS, incubated in 2 $^{\circ}$  antibody 2 hours at room temperature (Supplementary Table 1), washed in 1 $\times$  PBS, and when needed (Supplementary Table 1) incubated in Vector ABC (Vector Laboratories) for 3 hours, washed in 1 $\times$  PBS and labeled with TSA (Fluorescein or Cy3; PerkinElmer) for 10 minutes. Slides were washed in PBS, post-fixed in 4% PFA, incubated with 0.4 $\mu\text{g}/\text{ml}$  Hoechst and mounted with Fluoromount-G (SouthernBiotech). Immunofluorescent sections were imaged on a Nikon AR1 confocal or Nikon Widefield CCD Microscope. Each confocal image is a composite of maximum projections, derived from stacks of optical sections.

### Quantification of Pax7 and GFP contribution

For analysis of satellite cell numbers, cross-sections from EDL, TA, gastrocnemius, plantaris, soleus, EOM and diaphragm muscles from control (*Pax7<sup>+/+</sup>;Rosa<sup>DTA/+</sup>*) and satellite cell-ablation (*Pax7<sup>CreERT2/+</sup>;Rosa<sup>DTA/+</sup>*) cohorts were immunofluorescently labeled with Pax7. All Pax7<sup>+</sup> nuclei were counted by hand (observer blinded to genotype and age), and divided by the muscle volume for each section. Volume was determined from the whole muscle cross-sectional area (using ImageJ Analyze Particles function) multiplied by the thickness of the section.

To quantify satellite cell contribution to myofibers in *Pax7<sup>CreERT2/+</sup>;Rosa<sup>mTmG/+</sup>* mice, we immunofluorescently labeled sections for Tomato, GFP, and Hoechst and adjacent sections with MyHCI and laminin to identify slow (MyHCI<sup>+</sup>) and fast (MyHCI<sup>-</sup>) myofibers. All sections were imaged with identical exposure times and then green levels were adjusted identically in Photoshop based on levels in control *Pax7<sup>CreERT2/+</sup>;Rosa<sup>mTmG/+</sup>* mice

(without tamoxifen and excluding obvious GFP+ myofibers). Only myofibers with membrane-bound GFP were counted. To quantify the percentage of GFP+ myofibers, we counted all myofibers within each muscle, and subsequently counted GFP+ fibers. For the gastrocnemius, only the lateral and intermediate muscle heads were counted, and for the diaphragm, a region containing 100 slow fibers was counted. These images were then overlaid with images from adjacent sections labeled with MyHCI and laminin to identify GFP+ slow or fast fibers (soleus and diaphragm only). All images were counted by hand, with observer blinded to age or genotype. To determine whether individual 20 month mice had higher or lower GFP contribution across the majority of muscles, we recorded the percentile rank of the %GFP+ myofibers in each animal in each muscle. These percentile ranks across the 7 muscles for an individual mouse were used to perform t-tests (with Bonferroni correction) between animals.

### Quantification of myofiber cross-sectional area (CSA)

For analysis of myofiber CSA, we immunofluorescently labeled sections with laminin to identify myofiber borders and MyHCI to identify slow myofibers in 12 and 20 month cohorts of control *Pax7<sup>+/+</sup>;Rosa<sup>DTA/+</sup>* and satellite-cell ablated *Pax7<sup>CreERT2/+</sup>;Rosa<sup>DTA/+</sup>* mice. Myofiber CSA was quantified via MuscleQNT (developed by SF and MY and available at <https://github.com/stevendflygare/muscleQNT>). MuscleQNT works by first applying an adaptive thresholding method to locate muscle fibers and then uses steps of erosion and dilation to isolate individual muscle fibers. The adaptive thresholding, erosion, and dilation steps are parametric, and parameters used to score images were determined empirically (blinded to control or experimental status) for each cohort of muscles so as to best outline and isolate individual myofibers (parameters are listed in Supplementary Table 2). For comparison of 12 and 20 month control muscles (Figure 3), 12 month parameters were used (though 20 month parameters used on the same data showed identical trends, but with slightly different absolute values for fiber sizes). When using MuscleQNT, it is essential to do pairwise comparison of data sets, using exactly the same input parameters (erosion, box size, off set, minimum and maximum fiber size, Supplementary Table 2) as absolute CSA values are dependent upon the input parameters. Once fibers are located and isolated in an image, the size of each fiber is assigned as the number of pixels it occupies. In addition, myofibers were identified as slow myofibers if more than x% (x can be specified) of a fiber's pixels overlap MyHCI+ pixels (colocalization function). Fiber sizes of each image are written to an output file and summary statistics generated for each image. From this data, histograms are generated comparing the distribution of myofibers between 12 and 20 month muscles of control and satellite cell ablated muscles. To determine the significance of differences between 12 and 20 month or control and satellite cell ablated muscles, permutation tests were conducted. For permutation tests, the 12 or 20 month (or control or mutant) status of the mice were randomly permuted and myofibers were randomly sampled from each of the 12/20 month (or control/mutant) mice. The observed differences in each histogram bin between the counts of the 12 and 20 month (or control and mutant) mice were recorded and compared to the differences in the corresponding histogram bins of the original 12 and 20 month (or control and mutant) mice. The relative proportion of times a permuted difference is as great or greater than the observed difference in a specific

histogram bin allows us to determine for a specific histogram bin the significance of the observed difference in the counts between 12 and 20 month (or control and mutant) mice.

In addition to the analysis of the distribution of myofiber sizes, we also used a hierarchical linear regression model with a random effect to model the effect of mouse age and control/mutant status on muscle fiber size. The model leverages a random effect to control for intra-class correlation among myofibers that come from the same animal.

### Quantification of myonuclei

The number of myonuclei per fiber for control *Pax7<sup>+/+</sup>;Rosa<sup>DTA/+</sup>* and satellite-cell ablated *Pax7<sup>CreERT2/+</sup>;Rosa<sup>DTA/+</sup>* mice for 12 and 20 month cohorts was determined using EDL, diaphragm, and plantaris cross-sections stained with laminin and Hoechst. Myonuclei were identified by their location inside the basal lamina and the number of myonuclei was counted (by an individual blinded as to section genotype and age) in 150–250 EDL myofibers, 250–450 diaphragm myofibers, and 350–525 plantaris myofibers.

Myonuclear counts in cross-section can over-represent myonuclear number if myonuclei significantly change shape. To correct for this, we used a formula<sup>42</sup> that takes into account the observed myonuclear length in each muscle at either 12 or 20 months. We present our data as the number of myonuclei per mm of fiber length by **Equation 1:  $x = N*L/(l_m + d)$** , where  $x$  is the number of myonuclei in a fiber segment of length  $L$  (in our case, 1mm),  $N$  is the number of nuclei per myofiber in cross-section,  $l_m$  is the average myonuclear length at 12 or 20 months, and  $d$  is the thickness of the section.

Myonuclear length was determined using longitudinal sections of the diaphragm and EDL (myonuclear length for EDL was used for EDL and plantaris) from *Pax7<sup>CreERT2/+</sup>;Rosa<sup>mTmG/+</sup>* mice harvested at 12 or 20 months. Sections were immunofluorescently labeled with GFP, laminin and Hoechst and imaged on a Nikon AR1 confocal. Optical stacks were rendered in FluoRender<sup>55</sup>. Myonuclei were identified by their location inside the basal lamina and measured end-to-end using FluoRender. For each cohort, 30 nuclei per field were analyzed and average myonuclear length was determined.

### Supplementary Material

Refer to Web version on PubMed Central for supplementary material.

### ACKNOWLEDGEMENTS

We thank M.M. Murphy for technical advice, L.K. McLoon, and C.A. Peterson for helpful discussions, D.D. Cornelison and A.J. Merrell for critiques of the manuscript, and C. Rodesch and the Imaging Facility for microscopy support. Development of MuscleQNT by S.F. and M.Y. was supported by NIH R01GM088269 to MY. A.C.K was supported by NIH Hematology Grant (T32 DK007115) and M.P.C was supported by NIH Developmental Biology Grant (T32 HD07491). This work was supported by NIH R01 HD053728 and MDA 130903 to GK.

### REFERENCES

1. Narici MV, Maffulli N. Sarcopenia: characteristics, mechanisms and functional significance. *Br Med Bull.* 2010; 95:139–159. [PubMed: 20200012]

2. Rosenberg IR. Summary comments. *The American journal of clinical nutrition*. 1989; 50:1231–1233.
3. Brack AS, Bildsoe H, Hughes SM. Evidence that satellite cell decrement contributes to preferential decline in nuclear number from large fibres during murine age-related muscle atrophy. *J Cell Sci*. 2005; 118:4813–4821. [PubMed: 16219688]
4. Rai M, Nongthomba U, Grounds MD. Skeletal muscle degeneration and regeneration in mice and flies. *Curr Top Dev Biol*. 2014; 108:247–281. [PubMed: 24512712]
5. Kadi F, Ponsot E. The biology of satellite cells and telomeres in human skeletal muscle: effects of aging and physical activity. *Scand J Med Sci Sports*. 2010; 20:39–48. [PubMed: 19765243]
6. Pallafacchina G, Blaauw B, Schiaffino S. Role of satellite cells in muscle growth and maintenance of muscle mass. *Nutr Metab Cardiovasc Dis*. 2012
7. Thornell LE. Sarcopenic obesity: satellite cells in the aging muscle. *Curr Opin Clin Nutr Metab Care*. 2011; 14:22–27. [PubMed: 21088571]
8. Lepper C, Partridge TA, Fan CM. An absolute requirement for Pax7-positive satellite cells in acute injury-induced skeletal muscle regeneration. *Development*. 2011; 138:3639–3646. [PubMed: 21828092]
9. Murphy M, Kardon G. Origin of vertebrate limb muscle: the role of progenitor and myoblast populations. *Curr Top Dev Biol*. 2011; 96:1–32. [PubMed: 21621065]
10. Sambasivan R, et al. Pax7-expressing satellite cells are indispensable for adult skeletal muscle regeneration. *Development*. 2011; 138:3647–3656. [PubMed: 21828093]
11. Fry CS, et al. Regulation of the muscle fiber microenvironment by activated satellite cells during hypertrophy. *FASEB J*. 2014; 28:1654–1665. [PubMed: 24376025]
12. McLoon LK, Rowe J, Wirtschafter J, McCormick KM. Continuous myofiber remodeling in uninjured extraocular myofibers: myonuclear turnover and evidence for apoptosis. *Muscle Nerve*. 2004; 29:707–715. [PubMed: 15116375]
13. Schmalbruch H, Lewis DM. Dynamics of nuclei of muscle fibers and connective tissue cells in normal and denervated rat muscles. *Muscle Nerve*. 2000; 23:617–626. [PubMed: 10716774]
14. Spalding KL, Bhardwaj RD, Buchholz BA, Druid H, Frisen J. Retrospective birth dating of cells in humans. *Cell*. 2005; 122:133–143. [PubMed: 16009139]
15. Bruusgaard JC, Liestol K, Gundersen K. Distribution of myonuclei and microtubules in live muscle fibers of young, middle-aged, and old mice. *J Appl Physiol* (1985). 2006; 100:2024–2030. [PubMed: 16497845]
16. Kawai M, Saito K, Yamashita H, Miyata H. Age-related changes in satellite cell proliferation by compensatory activation in rat diaphragm muscles. *Biomed Res*. 2012; 33:167–173. [PubMed: 22790216]
17. Verdijk LB, et al. Satellite cells in human skeletal muscle; from birth to old age. *Age (Dordr)*. 2014; 36:545–547. [PubMed: 24122288]
18. Collins CA, et al. Stem cell function, self-renewal, and behavioral heterogeneity of cells from the adult muscle satellite cell niche. *Cell*. 2005; 122:289–301. [PubMed: 16051152]
19. Düsterhöft S, Yablonka-Reuveni Z, Pette D. Characterization of myosin isoforms in satellite cell cultures from adult rat diaphragm, soleus and tibialis anterior muscles. *Differentiation*. 1990; 45:185–191. [PubMed: 2090520]
20. Gibson MC, Schultz E. The distribution of satellite cells and their relationship to specific fiber types in soleus and extensor digitorum longus muscles. *Anat Rec*. 1982; 202:329–337. [PubMed: 7072981]
21. Kallestad KM, et al. Sparing of extraocular muscle in aging and muscular dystrophies: a myogenic precursor cell hypothesis. *Exp. Cell Res*. 2011; 317:873–885. [PubMed: 21277300]
22. Shefer G, Van de Mark DP, Richardson JB, Yablonka-Reuveni Z. Satellite-cell pool size does matter: defining the myogenic potency of aging skeletal muscle. *Dev Biol*. 2006; 294:50–66. [PubMed: 16554047]
23. Brack AS, Rando TA. Intrinsic changes and extrinsic influences of myogenic stem cell function during aging. *Stem cell reviews*. 2007; 3:226–237. [PubMed: 17917136]

24. Brooks SV, Faulkner JA. Contractile properties of skeletal muscles from young, adult and aged mice. *The Journal of physiology*. 1988; 404:71–82. [PubMed: 3253447]
25. Sousa-Victor P, et al. Geriatric muscle stem cells switch reversible quiescence into senescence. *Nature*. 2014; 506:316–321. [PubMed: 24522534]
26. Shavlakadze T, McGeachie J, Grounds MD. Delayed but excellent myogenic stem cell response of regenerating geriatric skeletal muscles in mice. *Biogerontology*. 2010; 11:363–376. [PubMed: 20033288]
27. Agbulut O, Noirez P, Beaumont F, Butler-Browne G. Myosin heavy chain isoforms in postnatal muscle development of mice. *Biol Cell*. 2003; 95:399–406. [PubMed: 14519557]
28. Bloemberg D, Quadrilatero J. Rapid determination of myosin heavy chain expression in rat, mouse, and human skeletal muscle using multicolor immunofluorescence analysis. *PLoS One*. 2012; 7:e35273. [PubMed: 22530000]
29. Porter JD. Extraocular muscle: cellular adaptations for a diverse functional repertoire. *Annals of the New York Academy of Sciences*. 2002; 956:7–16. [PubMed: 11960789]
30. Stuelsatz P, Keire P, Almuly R, Yablonka-Reuveni Z. A contemporary atlas of the mouse diaphragm: myogenicity, vascularity, and the Pax3 connection. *The journal of histochemistry and cytochemistry : official journal of the Histochemistry Society*. 2012; 60:638–657. [PubMed: 22723526]
31. White RB, Bierinx AS, Gnocchi VF, Zammit PS. Dynamics of muscle fibre growth during postnatal mouse development. *BMC Dev Biol*. 2010; 10:21. [PubMed: 20175910]
32. Seale P, et al. Pax7 is required for the specification of myogenic satellite cells. *Cell*. 2000; 102:777–786. [PubMed: 11030621]
33. Muzumdar MD, Tasic B, Miyamichi K, Li L, Luo L. A global double-fluorescent Cre reporter mouse. *Genesis*. 2007; 45:593–605. [PubMed: 17868096]
34. Blaveri K, et al. Patterns of repair of dystrophic mouse muscle: studies on isolated fibers. *Dev Dyn*. 1999; 216:244–256. [PubMed: 10590476]
35. Kinoshita I, Vilquin JT, Asselin I, Chamberlain J, Tremblay JP. Transplantation of myoblasts from a transgenic mouse overexpressing dystrophin produced only a relatively small increase of dystrophin-positive membrane. *Muscle Nerve*. 1998; 21:91–103. [PubMed: 9427228]
36. Cristea A, et al. Effects of aging and gender on the spatial organization of nuclei in single human skeletal muscle cells. *Aging Cell*. 2010; 9:685–697. [PubMed: 20633000]
37. Lexell J, Taylor CC, Sjöström M. What is the cause of the ageing atrophy? Total number, size and proportion of different fiber types studied in whole vastus lateralis muscle from 15- to 83-year-old men. *J Neurol Sci*. 1988; 84:275–294. [PubMed: 3379447]
38. Greising SM, Mantilla CB, Gorman BA, Ermilov LG, Sieck GC. Diaphragm muscle sarcopenia in aging mice. *Experimental gerontology*. 2013; 48:881–887. [PubMed: 23792145]
39. Murphy M, et al. Transiently active Wnt/b-catenin signaling is not required but must be silenced for stem cell function during muscle regeneration. *Stem Cell Reports*. 2014; 3
40. Wu S, Wu Y, Capecchi MR. Motoneurons and oligodendrocytes are sequentially generated from neural stem cells but do not appear to share common lineage-restricted progenitors in vivo. *Development*. 2006; 133:581–590. [PubMed: 16407399]
41. Murphy MM, Lawson JA, Mathew SJ, Hutcheson DA, Kardon G. Satellite cells, connective tissue fibroblasts and their interactions are crucial for muscle regeneration. *Development*. 2011; 138:3625–3637. [PubMed: 21828091]
42. Schmalbruch H, Hellhammer U. The number of nuclei in adult rat muscles with special reference to satellite cells. *Anat Rec*. 1977; 189:169–175. [PubMed: 911042]
43. Rodgers JT, et al. mTORC1 controls the adaptive transition of quiescent stem cells from G0 to G(Alert). *Nature*. 2014; 510:393–396. [PubMed: 24870234]
44. McLoon LK, Wirtschafter J. Activated satellite cells are present in uninjured extraocular muscles of mature mice. *Transactions of the American Ophthalmological Society*. 2002; 100:119–123. discussion 123–114. [PubMed: 12545684]
45. Hebert SL, Daniel ML, McLoon LK. The role of Pitx2 in maintaining the phenotype of myogenic precursor cells in the extraocular muscles. *PLoS One*. 2013; 8:e58405. [PubMed: 23505501]

46. Gage PJ, Suh H, Camper SA. Dosage requirement of Pitx2 for development of multiple organs. *Development*. 1999; 126:4643–4651. [PubMed: 10498698]
47. Kitamura K, et al. Mouse Pitx2 deficiency leads to anomalies of the ventral body wall, heart, extra- and periocular mesoderm and right pulmonary isomerism. *Development*. 1999; 126:5749–5758. [PubMed: 10572050]
48. Sambasivan R, et al. Distinct regulatory cascades govern extraocular and pharyngeal arch muscle progenitor cell fates. *Dev Cell*. 2009; 16:810–821. [PubMed: 19531352]
49. Zhou Y, et al. An altered phenotype in a conditional knockout of Pitx2 in extraocular muscle. *Invest Ophthalmol Vis Sci*. 2009; 50:4531–4541. [PubMed: 19407022]
50. Marzetti E, et al. Effects of short-term GH supplementation and treadmill exercise training on physical performance and skeletal muscle apoptosis in old rats. *Am J Physiol Regul Integr Comp Physiol*. 2008; 294:R558–R567. [PubMed: 18003794]
51. Rice KM, Blough ER. Sarcopenia-related apoptosis is regulated differently in fast- and slow-twitch muscles of the aging F344/N × BN rat model. *Mechanisms of ageing and development*. 2006; 127:670–679. [PubMed: 16678239]
52. Smith DO. Muscle-specific decrease in presynaptic calcium dependence and clearance during neuromuscular transmission in aged rats. *Journal of neurophysiology*. 1988; 59:1069–1082. [PubMed: 2836566]
53. Fry CS, et al. Inducible depletion of satellite cells in adult, sedentary mice impairs muscle regenerative capacity without affecting sarcopenia. *Nat Med*. 2015; 21:76–80. [PubMed: 25501907]
54. Reinert RB, et al. Tamoxifen-Induced Cre-loxP Recombination Is Prolonged in Pancreatic Islets of Adult Mice. *PLoS One*. 2012; 7:e33529. [PubMed: 22470452]
55. Wan Y, Otsuna H, Chien CB, Hansen C. An interactive visualization tool for multi-channel confocal microscopy data in neurobiology research. *IEEE transactions on visualization and computer graphics*. 2009; 15:1489–1496. [PubMed: 19834225]

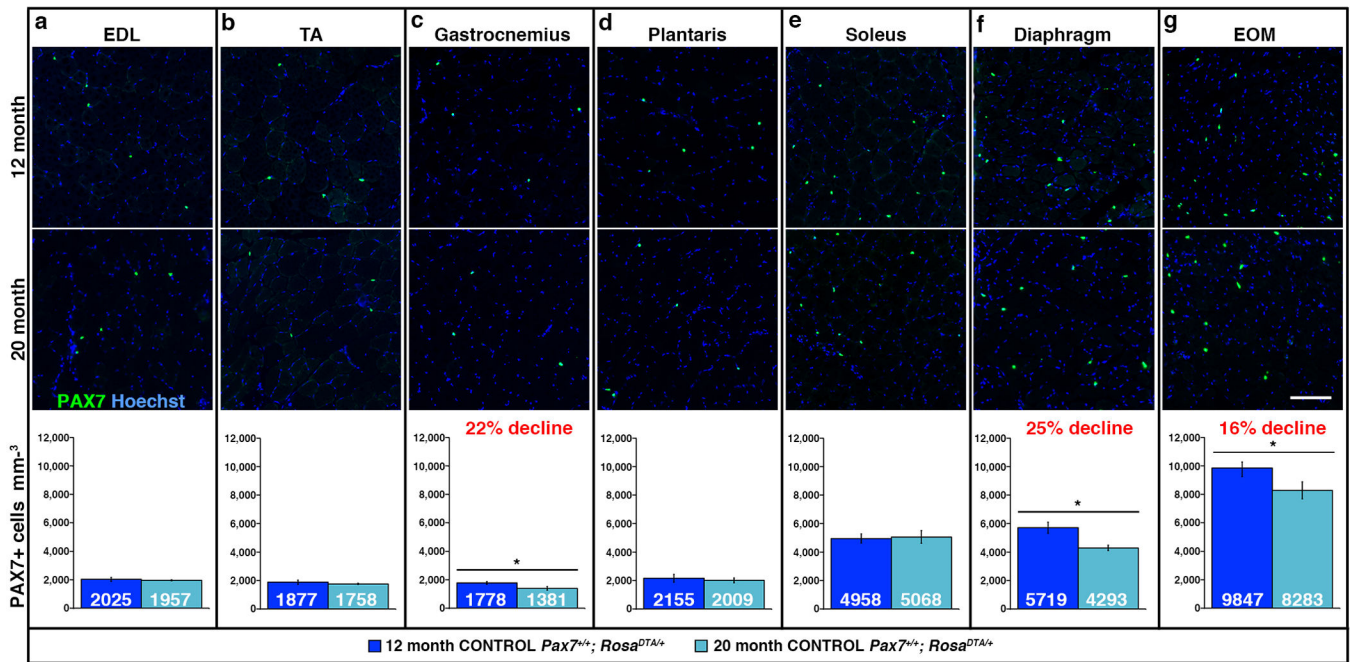


### Figure 1. Satellite cell number differs between muscles and with age

(a–g) Representative cross-sections showing Pax7+ satellite cells in EDL, TA, gastrocnemius, plantaris, soleus, diaphragm, and EOM at 12 and 20 months in control *Pax7<sup>+/+</sup>; Rosa<sup>DTA/+</sup>* mice. Scale bar = 100  $\mu$ m. Mean number of Pax7+ satellite cells per volume ( $\text{mm}^3$ ) of muscle at 12 months (dark blue, n = 6 EDL, TA, n = 7 other muscles) and 20 months (light blue, n = 3 EDL, n = 5 other muscles). Data are expressed as mean  $\pm$  1 s.e.m for all graphs. Two-tailed student *t*-test, \*p 0.05.

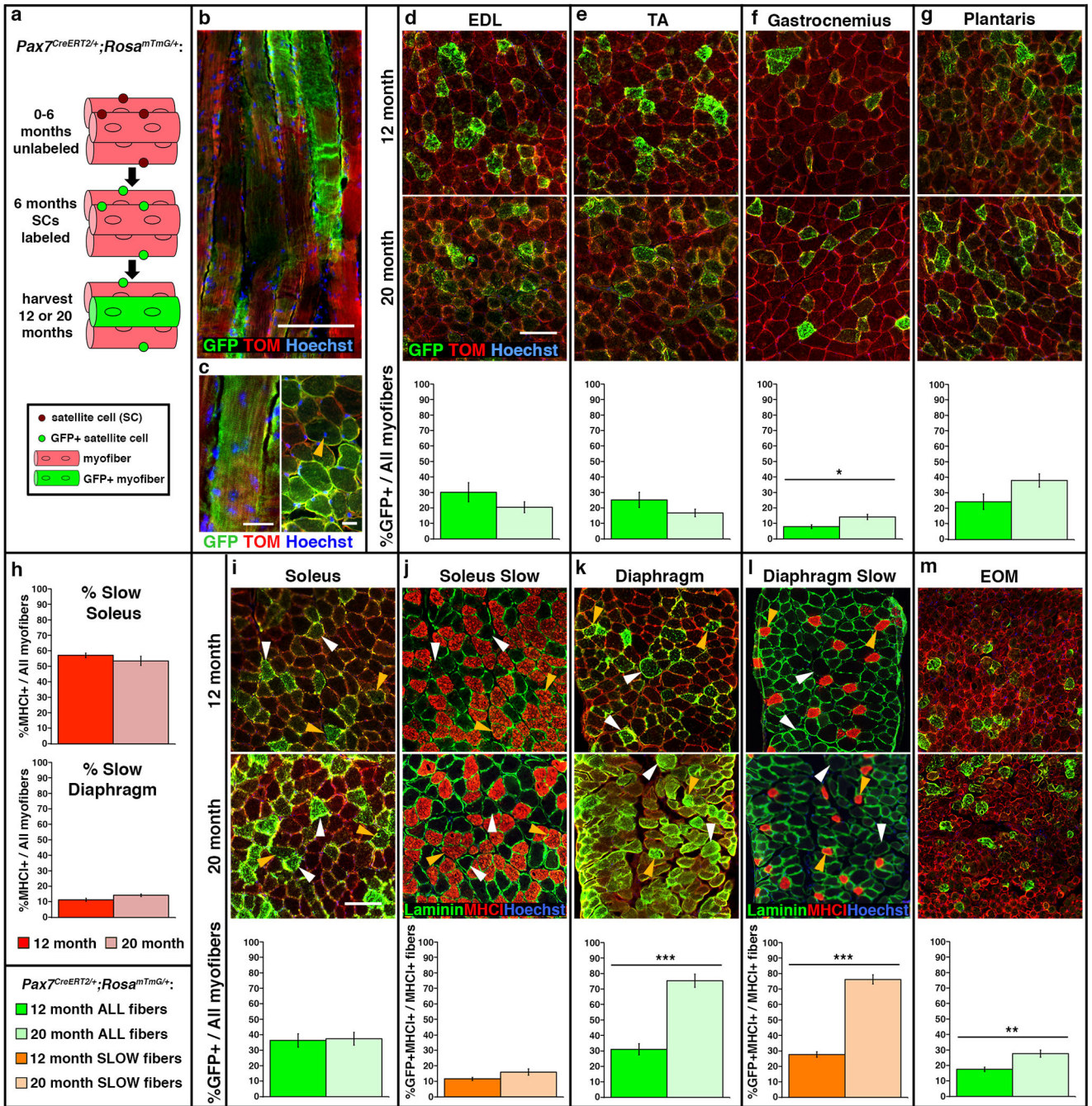


**Figure 2. Satellite cells contribute to myofibers in all muscles**

(a) Schematic showing genetic labeling of satellite cells with GFP at 6 months and harvested at either 12 or 20 months. (d–i, k, m) Representative cross-sections of EDL, TA, gastrocnemius, plantaris, soleus, diaphragm, and EOM of 12 or 20 month *Pax7<sup>CreERT2/+</sup>;Rosa<sup>mTmG/+</sup>* mice showing GFP+ myofibers to which satellite cells have contributed. It should be noted that the percentage of satellite cell contribution may be inflated in EOM due to the small size of its myofibers, which may reduce dilution of the GFP signal. Scale bar = 100  $\mu$ m. (j, l) Adjacent sections in soleus and diaphragm identifying



slow MyHCI+ myofibers. White arrows indicate fast GFP+MyHCI–fibers, orange arrows indicate slow GFP+MyHCI+ fibers. Green graphs show %GFP+ myofibers at 12 months (dark green, n = 4 for each muscle) or 20 months (light green, n = 6 for each muscle). Orange graphs show %GFP+ MyHCI+ myofibers in soleus (dark orange, n = 4 at 12 months; light orange, n = 6 at 20 months) and diaphragm (dark orange, n = 3 at 12 months; light orange, n = 5 at 20 months). Data are expressed as mean  $\pm$  1 s.e.m for all graphs. Two-tailed student *t*-test, \*p 0.05, \*\*p<0.01 \*\*\*p<0.001.

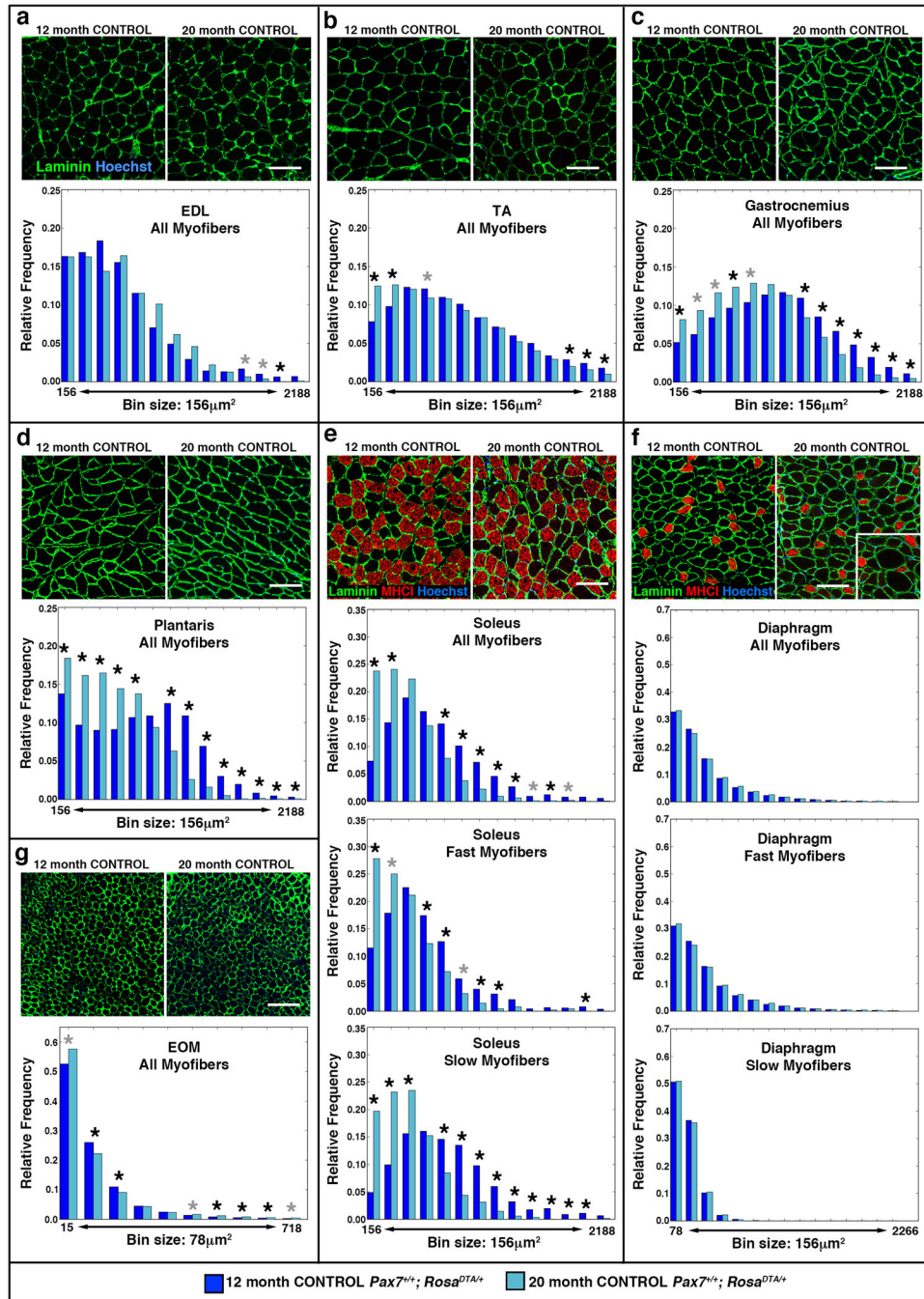


**Figure 3. Myofibers decline in size in most limb muscles with age**

(a–g) Representative cross-sections showing outlined laminin+ myofibers in EDL, TA, gastrocnemius, plantaris, soleus, diaphragm, and EOM at 12 and 20 months in control *Pax7*<sup>+/+</sup>; *Rosa*<sup>DTA/+</sup> mice. Slow MyHCI+ fibers (red) are identified in (e) soleus and (f) diaphragm. Scale bar = 100  $\mu\text{m}$  for all panels. Histograms generated by MuscleQNT show relative frequency of myofibers sizes in muscles at 12 months (dark blue, n = 7 for each muscle) and 20 months (light blue, n = 4 for EDL, n = 5 for other muscles). Additional histograms for (e) soleus and (f) diaphragm show relative frequency of fast MyHCI– and

slow MyHCI+ myofibers in muscles at 12 and 20 months. Permutation tests were conducted to determine whether counts of myofibers were significantly different in a particular bin between 12 and 20 month muscles (see Methods). Black asterisks indicate an empirical p value of <0.05 and gray asterisks a value of <0.10 (see Methods).

Author Manuscript

Author Manuscript

Author Manuscript

Author Manuscript

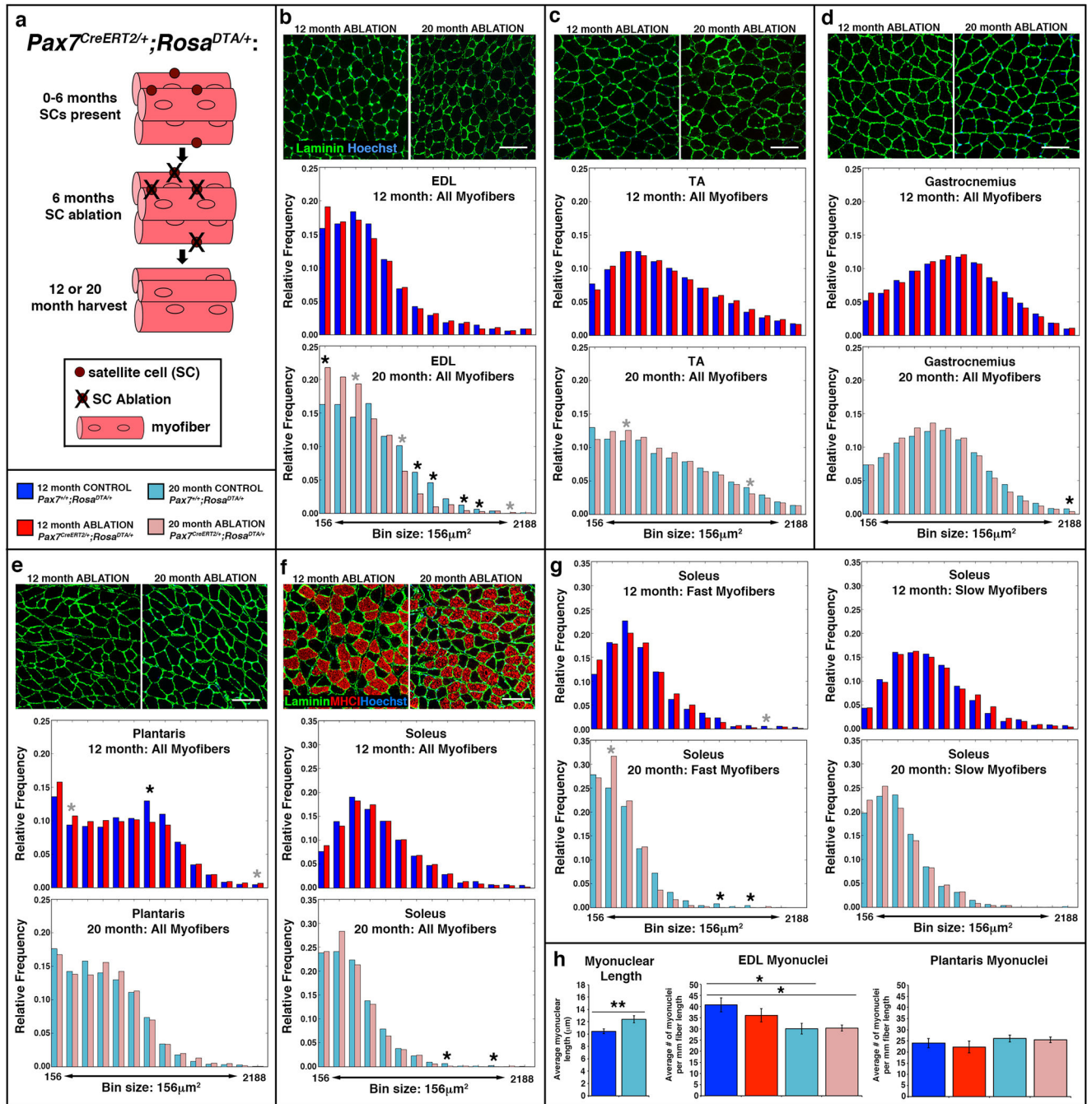


**Figure 4. Testing satellite cell role in maintaining size of limb myofibers**

(a) Schematic showing ablation of satellite cells at 6 months and harvested at either 12 or 20 months. (b–f) Representative cross-sections showing outlined laminin+ myofibers in limb muscles EDL, TA, gastrocnemius, plantaris, and soleus at 12 and 20 months in *Pax7<sup>CreERT2/+</sup>; Rosa<sup>DTA/+</sup>* mice (see Figure 3 for representative cross-sections of *Pax7<sup>+/+</sup>; Rosa<sup>DTA/+</sup>* mice). Histograms generated by MuscleQNT show relative frequency of myofiber sizes in muscles at 12 months (dark blue, control *Pax7<sup>+/+</sup>*, n = 7, for each muscle; red satellite cell ablated *Pax7<sup>CreERT2/+</sup>*, n = 8 for each muscle) and 20 months (light blue,

control *Pax7<sup>+/+</sup>*, n = 4 for EDL, n = 5 for other muscles; pink, satellite cell ablated *Pax7<sup>creERT2/+</sup>*, n = 6 for each muscle). Scale bar = 100  $\mu$ m for all panels. **(g)** Additional histograms for the soleus show frequency of fast MyHCI<sup>-</sup> and slow MyHCI<sup>+</sup> myofibers. Permutation tests (see Methods) were conducted to determine whether counts of myofibers were significantly different in a particular bin between control and satellite cell ablated muscles. Black asterisks indicate an empirical p value of <0.05 and gray asterisks a value of <0.10 (see Methods). Note that the MuscleQNT parameters slightly differ between 12 and 20 month TA, gastrocnemius, plantaris, and diaphragm muscles; to explicitly compare the CSA of 12 and 20 month control of muscles see Figure 3. **(h)** Myonuclei are significantly longer (two-tailed student *t*-test, \*\*p<0.01) and number of myonuclei are significantly reduced in 20 month versus 12 month EDL, but not in plantaris (two-tailed student *t*-test, \*p<0.05).

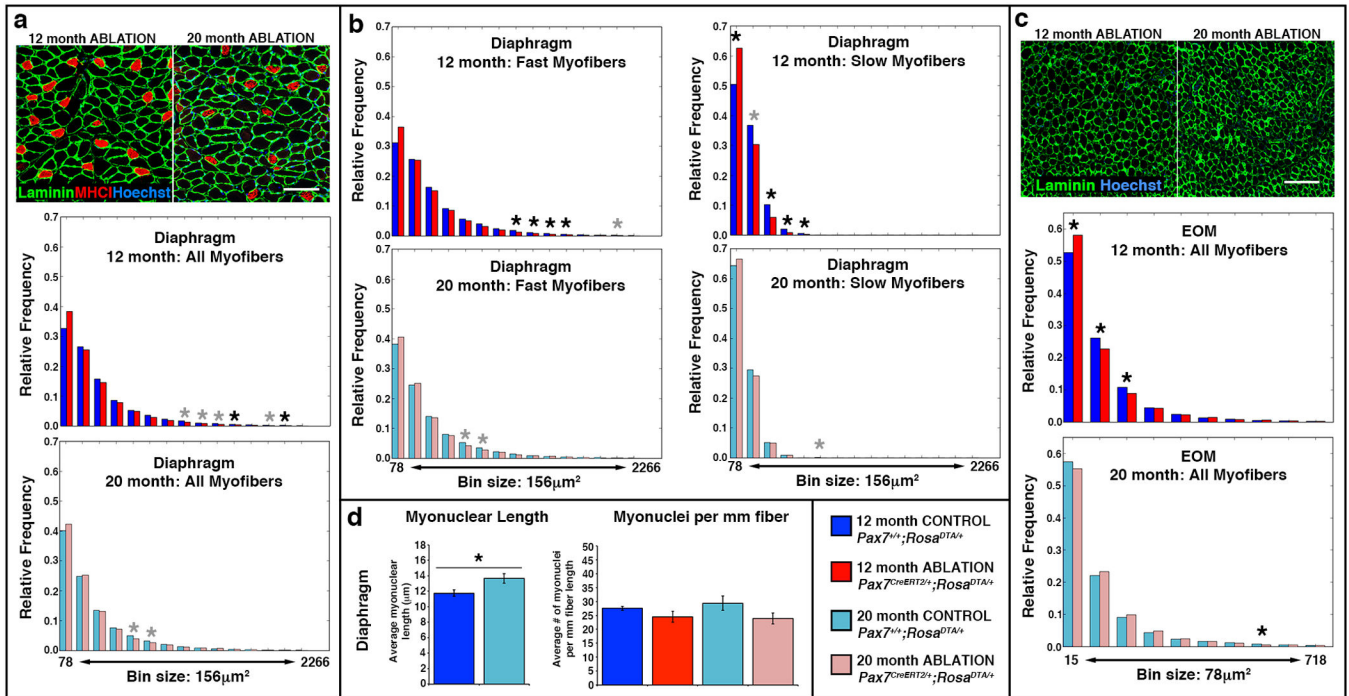


### Figure 5. Testing satellite cell role in maintaining EOM and diaphragm myofibers

**(a, c)** Representative cross-sections showing outlined laminin+ myofibers in diaphragm and EOM at 12 and 20 months in *Pax7<sup>CreERT2/+</sup>;Rosa<sup>DTA/+</sup>* mice (see Figure 3 for representative cross-sections of *Pax7<sup>+/+</sup>;Rosa<sup>DTA/+</sup>* mice). Histograms generated by MuscleQNT show relative frequency of myofibers sizes in muscles at 12 months (dark blue, control *Pax7<sup>+/+</sup>*, n = 7; red, satellite cell ablated *Pax7<sup>CreERT2/+</sup>*, n = 8) and 20 months (light blue, control *Pax7<sup>+/+</sup>*, n = 5, pink, satellite cell ablated *Pax7<sup>CreERT2/+</sup>*, n = 6) Scale bar = 100  $\mu\text{m}$  in both panels. **(b)** Additional histograms for the diaphragm show frequency of fast MyHC<sup>-</sup> and slow MyHC<sup>+</sup> myofibers. Permutation tests (see Methods) were conducted to determine whether counts of myofibers were significantly different in a particular bins between control and satellite cell ablated muscles. Black asterisks indicate an empirical p value of <0.05 and gray asterisks a value of <0.10 (see Methods). **(d)** Myonuclei are significantly longer at 12 months (two-tailed student *t*-test, \**p*<0.05), but number of myonuclei do not change between 12 and 20 months in the diaphragm (two-tailed student *t*-test).

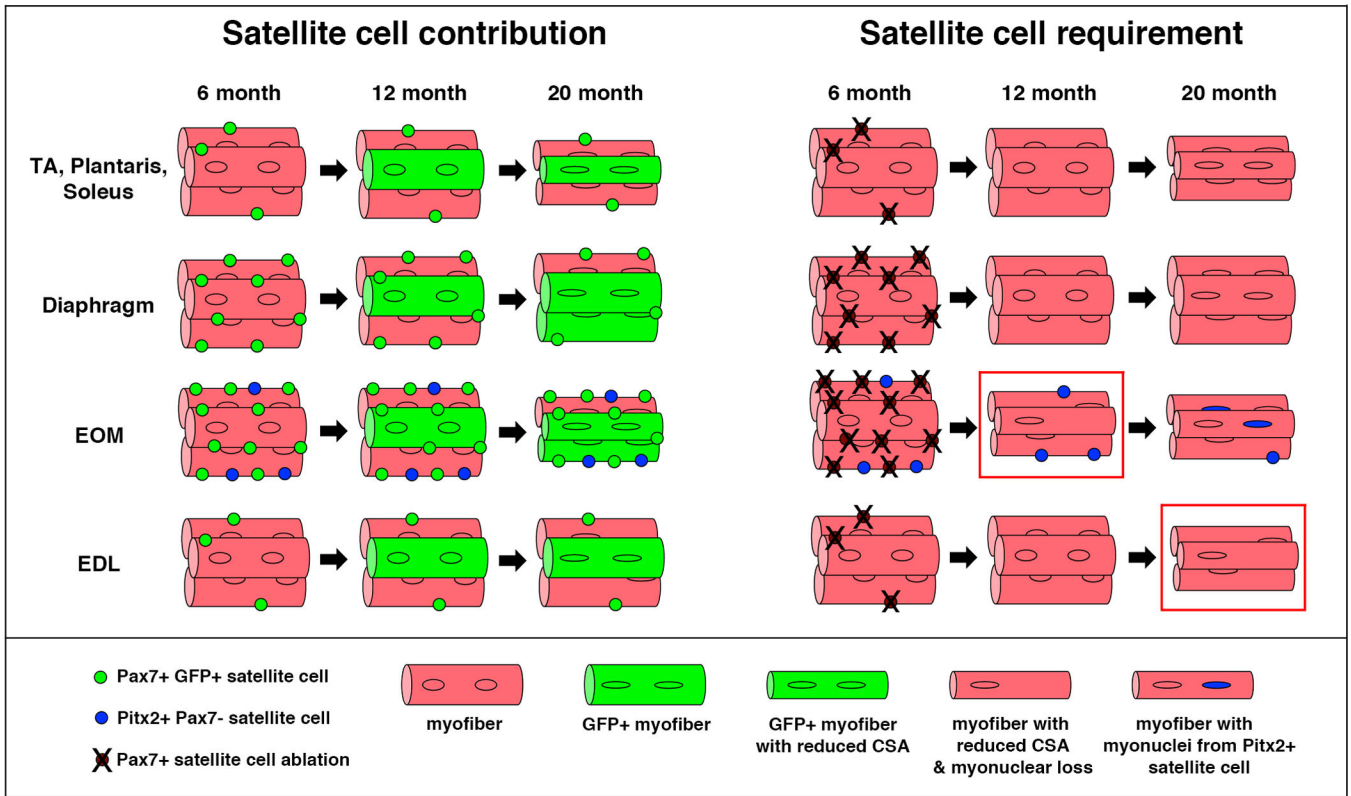


**Figure 6. Summary of satellite cell contribution to adult uninjured muscle**

Pax7+ satellite cells, labeled at 6 months, contribute to myofibers in all muscles between 6 and 12 months. After 12 months there is no appreciable satellite cell contribution in most limb muscles (TA, plantaris, soleus, and EDL), but there is continued contribution in the diaphragm and EOM (also gastrocnemius, not shown). Pax7+ satellite cells are not required to maintain myofiber cross-sectional area of most muscles, but may help maintain myofiber CSA in EOM at 12 months and EDL at 20 months (red boxes). In EOM potentially Pax7- Pitx2+ (blue circles) satellite cells, as suggested by<sup>45</sup>, compensate when Pax7+ satellites are ablated. Pax7+ satellite cells are shown as green circles in left panels and as brown circles in right panels.